

Chatter suppression in large overhang face milling using a toolholder with high dynamic performance

Yan Xia^{1,2}, Yi Wan^{1,2}, Xichun Luo³, Yanan Li^{1,2}, Zhanqiang Liu^{1,2}, Ning Gong⁴, Jinglong Cao⁴

¹ Key Laboratory of High Efficiency and Clean Mechanical Manufacture, Ministry of Education, School of Mechanical Engineering, Shandong University, Jinan, 250061, China

² National Demonstration Centre for Experimental Mechanical Engineering Education, Shandong University, Jinan, 250061, China

³ Centre for Precision Manufacturing, DMEM, University of Strathclyde, Glasgow, G1 1XJ, UK

⁴ Komatsu (Shan Dong) Construction Machinery Co., Ltd, Jining, 272073, China

Abstract: For the milling cutter, its large ratio of length to diameter usually requires to be used to machine box and shell parts, and this, combining with the feature of variable cross sections, also limits the improvement of stable machining region. The paper presents a method to enhance the chatter stability in this kind of milling operation by developing the damping cutters. Influence of modal parameters of the cutter on the limit cutting depth is investigated, and it is proven that increasing the dynamic stiffness can efficiently extend the stable zone. Subsequently, two damping cutters are designed by inlaying different strips and damping materials into the toolholder, and their modal characteristics are theoretically analyzed to reveal the relation among stiffness, loss factor and structural dimensions. The optimal structural dimensions are determined by the finite element method. Lastly, the two damping cutters are manufactured and then are verified by modal tests and milling experiments. Comparisons of the measured results show the effectiveness of the developed damping cutters.

Keywords: Milling cutter; ratio of length to diameter; variable cross sections; chatter stability; stiffness; loss factor

1. Introduction

Chatter is a harmful self-excited vibration, which affects the surface quality of the machined workpiece, and even damages the machine tools and cutter [1]. There have been a considerable amount of literature on chatter problem. Considering whether it is real-time, the existing methods can be classified into two kinds, i.e. in-process and out-of-process strategies [2].

The essence of the in-process strategy is to detect and identify the occurrence of chatter during machining process and then to adjust the cutting parameters so as to achieve the chatter-free condition [2, 3]. This kind of control strategy usually contains chatter detection and active control method. Due to the advantages of high efficiency and high accuracy, online chatter detection has been investigated widely. Various signals are used to identify chatter, such as force [4, 5], acceleration [6, 7], sound [8], etc. After signal acquisition, the feature extraction is vital to precisely detect chatter, where many relative signal processing methods, including variational mode decomposition [8], continuous wavelet transform [9], and convolutional neural network [10], are proposed. However, multiple sensors, signal acquisition and processing system, and other auxiliary devices are required, which hinders the wide application of chatter detection. On the other hand, the active control method becomes increasingly important in the field of chatter control thanks to its efficiency and flexibility. Accordingly, many active devices are developed, such as electromagnetic actuator [11], piezoelectric actuator [12], and magnetorheological fixture [13]. However, these devices usually need the elements of monitoring, identification and execution, which leads to the complex design and high cost of the active method.

As opposed to the in-process strategy, the out-of-process strategy is easy to implement. Stability prediction is a commonly effective way to avoid chatter, in which the predicted stability chart describes the relationship between speed and the stable limit to determine the suitable cutting parameters [14]. The solutions to calculate the stability chart are proposed, such as the discretization method [15-17] and frequency method [18]. In addition, the dynamic parameters and cutting force coefficient of the machining system obtained precisely is crucial to predict the stability chart. However, these parameters are not constant due to the time-varying characteristic of the machining process, which has negative influence on the stability prediction [19]. With the aim to suppress chatter better, the passive control method is investigated broadly. The essence of the passive control method is to improve the machining stability through introducing the additional device that can consume vibration energy or break the regeneration effect [3]. The passive equipment proposed is mainly composed of friction damper, vibration absorber, tuned mass damper, and constrained layer damper. For instance, Madoliat et al. [20] placed the core and multi-fingered cylinder into the axial

hold of a slender end milling tool to dissipate energy through the friction generating among them. The dynamic vibration absorber with variable stiffness was designed and was then filled into a boring bar, where the vibration reduction performance was verified by experiments [21]. A passive damper was developed and was embedded into a milling cutter to achieve the chatter control [22]. According to the constrained layer damping beam theory, a damping boring was proposed, and could significantly improve the machining stability [23].

From the references reviewed above, even though chatter control has been explored broadly, the milling dynamics has received very little attention with regard to the cutter with large ratio of length to diameter and variable cross sections. Therefore, the motivation of this paper is to study the dynamics of this kind of milling cutter, and then to design the damping cutter, thereby improving the corresponding stable machining zone.

2. Dynamic model of milling cutter

As shown in Figure 1, the milling cutter includes cutter head and toolholder with long overhang and variable cross sections. Supposing the positioning connection between spindle and toolholder is rigid, the milling cutter can be regarded as the cantilever structure with one end fixed and another end free.

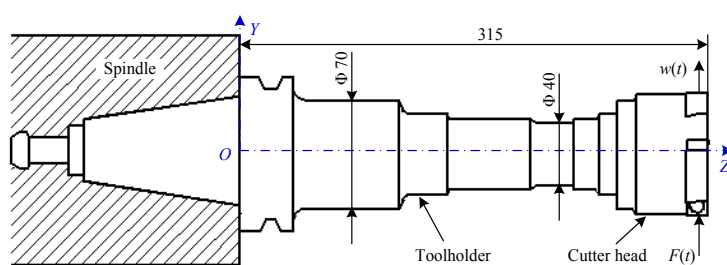


Figure 1. Schematic diagram of milling cutter. (The dimension units are mm)

During milling operation, the end free is subjected to the milling force. Note, that the axial force along z direction can be neglected, since it has little effect on the radial displacement. The cutter can be simplified as a cutter-spring-damper system. The milling forces attached on the cutter head and the corresponding displacement can meet the requirement of the following equation.

$$m \ddot{w}(t) + c \dot{w}(t) + k w(t) = F(t) \quad (1)$$

where m is mass, c is damping, k is the stiffness of the cutter, $F(t)$ is the exciting force produced from the cutting process. The damping c can be described as follows:

$$c = \eta\sqrt{km} \quad (2)$$

where η represents the loss factor of the cutter. Substituting Equation (2) into Equation (1), then the system response can be obtained, which is expressed by:

$$w(t) = \frac{F_0}{k} \cdot \frac{1}{\sqrt{(1-\nu^2)^2 + (\eta\nu)^2}} e^{i(\omega t - \psi)} \quad (3)$$

where F_0 represents the amplitude of $F(t)$, $\nu = \omega/\omega_n$ is the frequency ratio, ω_n stands for the natural frequency, ψ is the phase angle. According to Equation (3), it can be qualitatively obtained that the vibration displacement can be decreased with the increase of k and η . In order to further analyze the relation between the vibration response of the machining system and its modal characteristic in detail, the dynamic stiffness d is defined and can be expressed by:

$$d = \eta k \quad (4)$$

According to the dynamics theory of milling operation [18], the cutter in Figure 1 can be expressed as a vibration system as seen in Figure 2. Here, the milling force $F(t)$ is described as:

$$\{\mathbf{F}(t)\} = \frac{1}{2} a K_t [\mathbf{A}_0] \{\Delta(t)\} \quad (5)$$

with

$$\mathbf{F}(t) = \{F_x \quad F_y\}^T \quad \Delta(t) = \{\Delta x(t) \quad \Delta y(t)\}^T \quad (6)$$

where a refers to the cutting depth, $[\mathbf{A}_0]$ is the average directional coefficient matrix, K_t is the cutting force coefficients, $\Delta(t)$ represents the variation of vibration displacements.

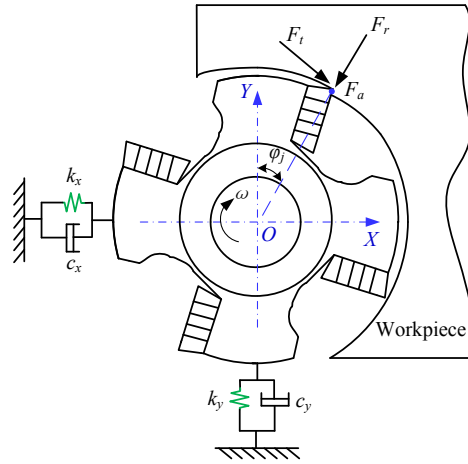


Figure 2. Dynamic model of milling cutter system.

Transforming Equation (5) from time domain to frequency domain leads to:

$$\{\mathbf{F}(\omega)\} = \frac{1}{2} a K_t [\mathbf{A}_0] (1 - e^{-i\omega T}) [\Phi(i\omega)] \{\mathbf{F}(\omega)\} \quad (7)$$

with

$$[\Phi(i\omega)] = \begin{bmatrix} \Phi_{xx}(i\omega) & 0 \\ 0 & \Phi_{yy}(i\omega) \end{bmatrix} \quad (8)$$

where $\Phi(i\omega)$ stands for the transfer function, and it can be described as:

$$\begin{aligned} \Phi_{xx}(i\omega) &= \frac{1}{k_x(1 - \nu^2 + i\eta_x \nu)} \\ \Phi_{yy}(i\omega) &= \frac{1}{k_y(1 - \nu^2 + i\eta_y \nu)} \end{aligned} \quad (9)$$

The cutter will be under the limit stable state at chatter frequency ω_c , and the corresponding characteristic equation can be derived as follows.

$$\det \left\{ [\mathbf{I}] - \frac{1}{2} a_{\text{lim}} K_t [\mathbf{A}_0] (1 - e^{-i\omega_c T}) [\Phi(i\omega_c)] \right\} = 0 \quad (10)$$

After solving Equation (10), the limit axial depth of cut a_{lim} and the corresponding speed Ω can be given by:

$$\begin{aligned} a_{\text{lim}} &= -\frac{2\pi}{NK_t} \left(\frac{\lambda_{\text{Re}}(1 - \cos(\omega_c T)) + \lambda_{\text{Im}} \sin(\omega_c T)}{1 - \cos(\omega_c T)} + i \frac{\lambda_{\text{Im}}(1 - \cos(\omega_c T)) - \lambda_{\text{Re}} \sin(\omega_c T)}{1 - \cos(\omega_c T)} \right) \\ \Omega &= \frac{60\omega_c}{N(\pi - 2 \arctan(\lambda_{\text{Im}}/\lambda_{\text{Re}}) + 2n\pi)} \quad n = 0, 1, 2, \dots \end{aligned} \quad (11)$$

where λ is the eigenvalue, N is the teeth number of the cutter. Based on Equations (4) and (11),

Figure 3 describes the relationship among limit axial depth of cut a_{lim} , dynamic stiffness d and spindle speed Ω . It can be clearly observed that a_{lim} can be increased significantly with the gradual increase of d , which means the improvement of chatter stability.

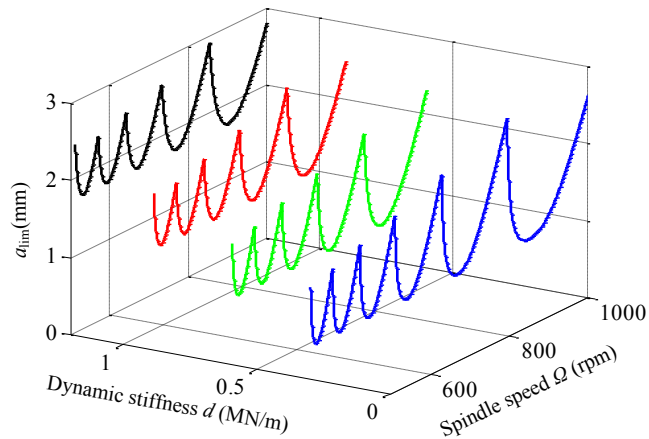
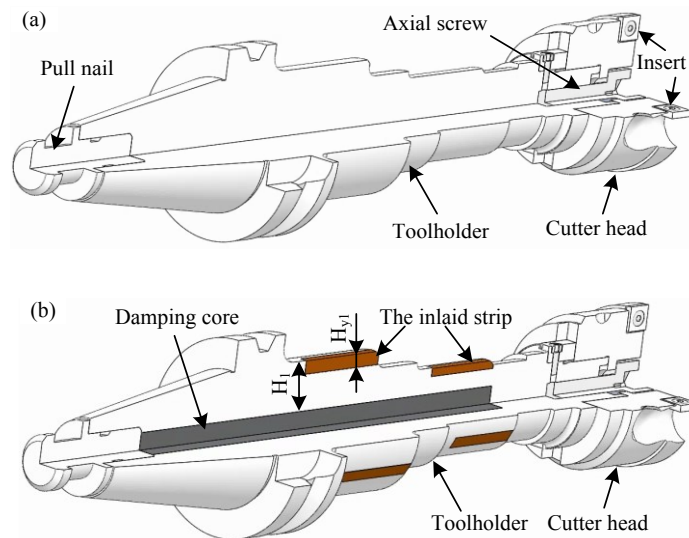


Figure 3. Stability charts under different dynamic stiffness.

3. Development of the damping cutter

3.1 Design of the damping cutter



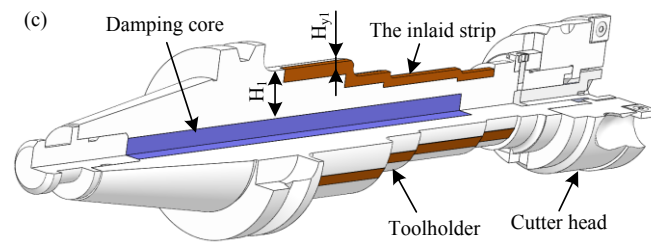


Figure 4. Comparison of structures for the conventional cutter (a), damping cutter with discontinuous strips (b) and damping cutter with continuous strips (c).

As shown in Figure 4a, the conventional cutter, named CC, is mainly composed of the conventional toolholder, cutter head, inserts, pull nail and axial screw. The cutter can be fixed with the spindle via the pull nail. The cutter head with four inserts is closely connected with the toolholder by the axial screw. Based on the external shape of the conventional toolholder, two damping cutters, named DCDS and DCCS respectively, are designed initially as seen in Figures 4b and 4c. The damping material is filled into the toolholder body to improve the damping performance, and the strips made of material with high modulus are embedded into the toolholder to increase the stiffness, which can enlarge the dynamic stiffness of the cutter. It should be pointed out that the strip embedded into the DCCS is integral, which matches with the external shape of the toolholder, while there exist two segments of the inlaid strip in the DCDS. The material of 35CrMo steel is used to manufacture the base body of the toolholder. Owing to its high damping property, Foamed aluminium (FA) and Polyurethane rubber (PR) are selected as the materials of the damping core in the DCDS and DCCS, respectively [4, 23]. And YG6 is selected to make the strip since it has high modulus. The properties of the materials used are given in Table 1.

Table 1. Material properties used in cutters.

Material	Density (g/cm ³)	Elastic modulus (GPa)	Poisson's ratio	Material loss factor (%)
35CrMo steel	7.87	213	0.29	0.1
YG6 carbide	14.5	600	0.21	0.1
FA	0.65	12	0.33	12
PR	1.11	30	0.3	47

3.2 Modal characteristic analysis of the damping cutter

As illustrated in Figure 3, the stability performance of the milling cutter is characterized by the

dynamic stiffness. In order to analyze the modal characteristic of the damping cutter, some assumptions are firstly provided as follows [24]: (1) the bending strains produced from damping core, strip or base body of the toolholder show the same linear distribution in vertical direction; (2) there is not relative sliding between the contact surfaces among different parts; (3) the material of damping core is uniform. Based on the dynamic model in Figure 1, the cutter is regarded as a cantilever structure [25], whose stiffness can be expressed by:

$$k = \frac{3(EI)_w}{L^3} \quad (12)$$

where L represents the overhang length of the cutter, $(EI)_w$ denotes the equivalent bending stiffness which can be described as:

$$(EI)_w = (EI)_1 + (EI)_2 \quad (13)$$

where $(EI)_1$ is the bending stiffness of base body and the strips, and $(EI)_2$ is the bending stiffness of damping core.

Substituting Equation (13) into Equation (12) yields

$$k = \frac{3\pi[D_2^4 \cdot E_2 + (D_1^4 - D_2^4) \cdot E_1]}{L^3} \quad (14)$$

where D_j and E_j ($j=1, 2$) are the external diameters and elastic modulus of the toolholder certain section and damping core, respectively.

During milling operation, the cutter is suffered from the milling vibration, where the damping core can dissipate the vibration energy by the resulted bending strain. Based on the bending strain energy method [24, 26], the loss factor of the damping cutter can be represented by:

$$\eta = \frac{\Delta W}{W} \quad (15)$$

where ΔW stands for the dissipation energy by damping core, and W is the total deformation energy of the cutter. Substituting the structural and material parameters of different parts of the damping cutter into Equation (15), then the following equation can be obtained:

$$\eta = \frac{\alpha\beta[H_{12}^2 + r_2^2(1 + 2\alpha)]}{\alpha H_{12}^2 + (\alpha r_2^2 + r_1^2)(1 + 2\alpha)} \quad (16)$$

with

$$r_1^2 = \frac{H_1^2}{12} \quad r_2^2 = \frac{H_2^2}{12} \quad H_{12} = \frac{H_1 + H_2}{2} \quad e = \frac{E_2}{E_1} \quad h = \frac{H_2}{H_1} \quad \alpha = e \cdot h \quad (17)$$

where H_1 is the thickness of base body of the toolholder, $H_2 = D_2/2$ is the thickness of damping core, β is the material loss factor. Thus, Equation (16) can be further transformed into the following expression:

$$\eta = \frac{eh(3 + 6h + 4h^2)}{1 + eh(5 + 6h + 4h^2)} \quad (18)$$

According to Equation (14) and Equation (18), the relation among modal characteristics of the damping cutter, its structural dimension and material property are analyzed as shown in Figure 5. When h increases, i.e. increasing the diameter of damping core, the stiffness gradually decreases, while the loss factor is enhanced remarkably. The e of large value has a positive effect on the modal characteristic. Apparently, when FA or PR is selected, e is equal to 0.06 and 0.14 respectively, which shows well influence on the damping performance. Therefore, it is imperative to determine the suitable structural dimension for the damping cutters.

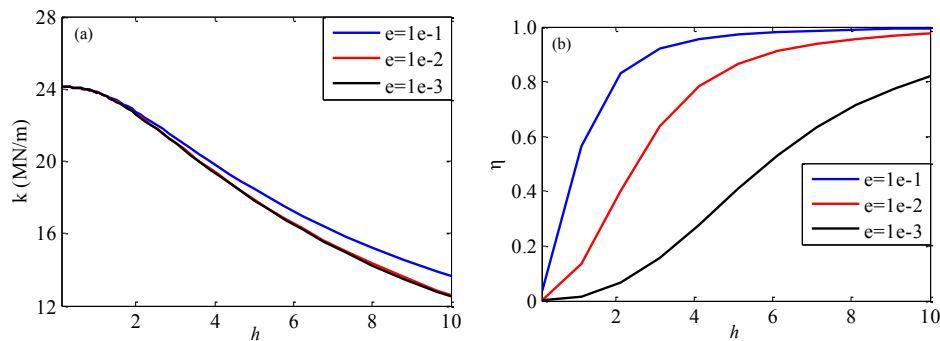


Figure 5. Stiffness (a) and loss factor (b) with respect to structural dimension and material property.

3.3 Parameter optimization and manufacture of the damping cutter

With consideration of the variable cross-sectional nature of the toolholder, it is essential to determine the optimum structural dimension of the damping core and strip by the finite element method. As seen in Figure 4, the thickness of the inlaid strip and the diameter of the damping core, i.e., H_{y1} and H_2 , are selected as the design variable. For convenience of the optimization analysis, the thickness of the strips embedded into the different cross sections of the toolholder are proportional to the corresponding dimeters of cross sections. The optimization goal is to make the maximum response amplitude of cutter head smallest. The basic flow of the optimization analysis

by using Workbench mainly includes: creating firstly the input and output channels in the cutter head, then setting the design variable and optimization goal, further conducting the optimized analysis by goal driven optimization, and finally achieving the solutions. The obtained optimal parameters for the two damping cutters are listed in Table 2. The corresponding dynamic stiffness and response amplitudes for three cutters are demonstrated in Figure 6. It can be seen that the dynamic characteristic of the DCDS is better than of the conventional cutter, while the dynamic performance of the DCCS is better than of the DCDS. According to the optimal design parameters, the two damping cutters are manufactured, which can be seen in Figure 7.

Table 2. Optimal design parameters

Number	Cutter	Design parameters	
		H _{y1} (mm)	H ₂ (mm)
1	CC	-	-
2	DCDS	10.26	15.45
3	DCCS	7.35	18.14

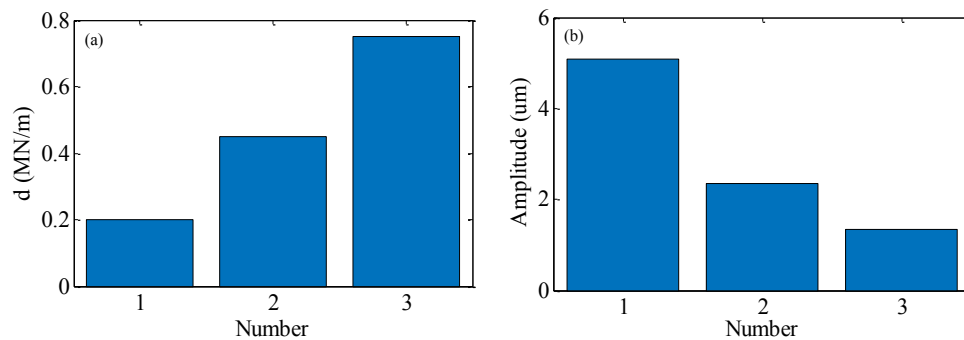


Figure 6. The simulated dynamic stiffness (a) and response amplitude (b) for the CC, DCDS and DCCS.

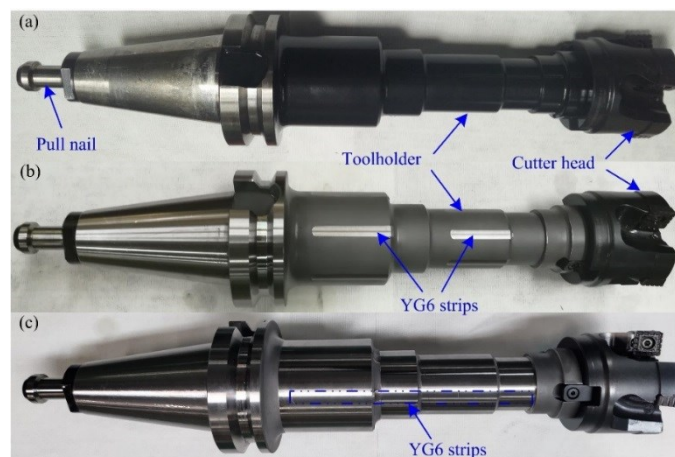


Figure 7. Photographs of the CC (a), DCDS (b) and DCCS (c).

4. Performance tests and comparison

In order to verify the damping cutters developed in Section 3, modal testing and milling experiments are conducted on a CNC machining center (SPN50R) in the workshop of KSD. Before milling tests, modal testing is performed to measure the modal parameters of the machining system for predicting the stability chart. The used cutter head with the diameter of 80 mm has four inserts. The material of ductile cast iron is used to make workpiece.

4.1 Modal testing

The hammer (CL-YD-303) with the sensitivity of 4.29 pC/N and accelerometer sensor (Dytran 3035B) are employed during modal testing as shown in Figure 8. The hammer provides the impact forces at the cutter head and synchronously the responses signals are collected by B&K Pulse 3560C data acquisition system. The measured frequency curves along y direction for three milling cutters are illustrated in Figure 9. The corresponding modal parameters are identified and given in Table 3, which experimentally shows the obvious improvement of dynamic stiffness for the damping cutters, comparing with the conventional cutter.

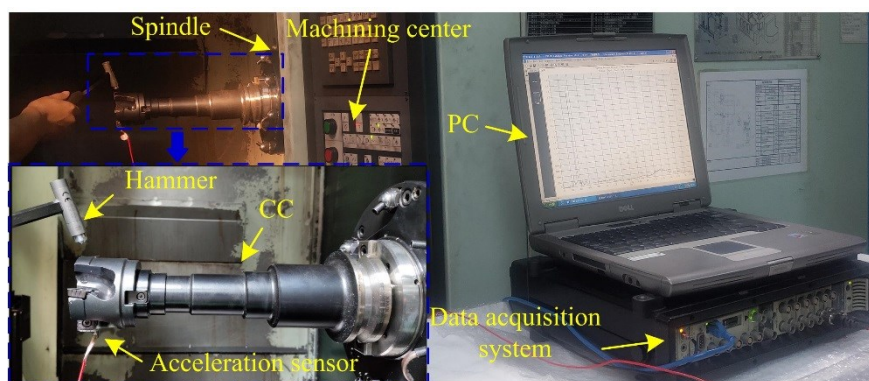


Figure 8. Experimental setup of modal tests.

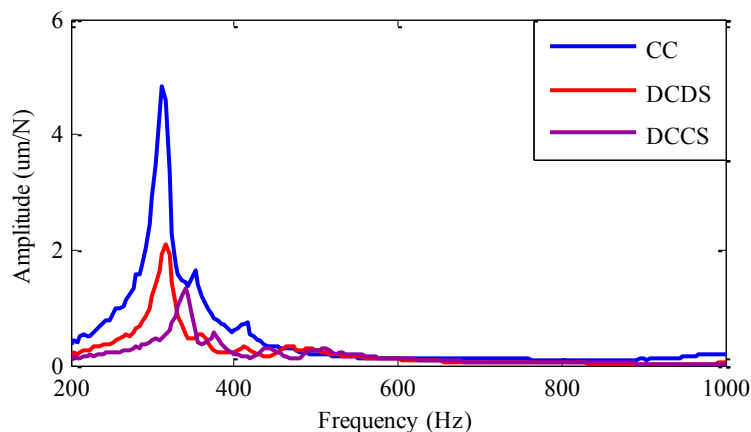


Figure 9. Measured frequency curves of the CC, DCDS and DCCS.

Table 3. Measured modal parameters of three cutters

Modal parameters	CC	DCDS	DCCS
Natural frequency (Hz)	312	316	340
Damping ratio (%)	1.28	2.53	2.35
Stiffness (MN/m)	8.07	9.3	16.08
Dynamic stiffness (MN/m)	0.21	0.47	0.76

4.2 Face milling experiments

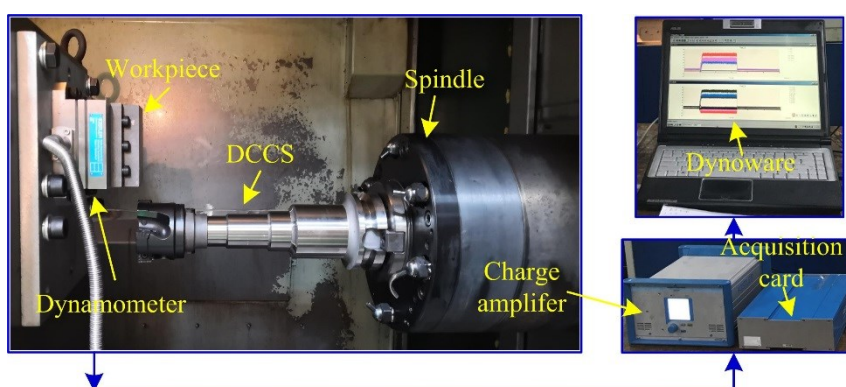


Figure 10. Experimental setup of milling force tests.

Figure 10 presents the cutting experimental setup for three milling cutters. The workpiece is mounted on the dynamometer (Kistler 9257B) fixed on the vertical machine table. Thereby, the milling forces can be measured to detect the cutting state during milling process. The cutting parameters of the conventional cutter actually adopted in workshop are spindle speed of 796 rpm, axial depth of cut of 1.5 mm and feed rate of 31 mm/min. In order to compare the machining stable

performance for CC, DCDS and DCCS, three axial depths of cut are chosen, including 1 mm, 1.5 mm and 2 mm, and other machining parameters are constant. The measured machining state from the experimental results are exhibited in the predicted stability charts in Figure 11. Meantime, the spectra of the milling forces for three cutters under different axial depth of cut are presented in Figures 12-14 in detail.

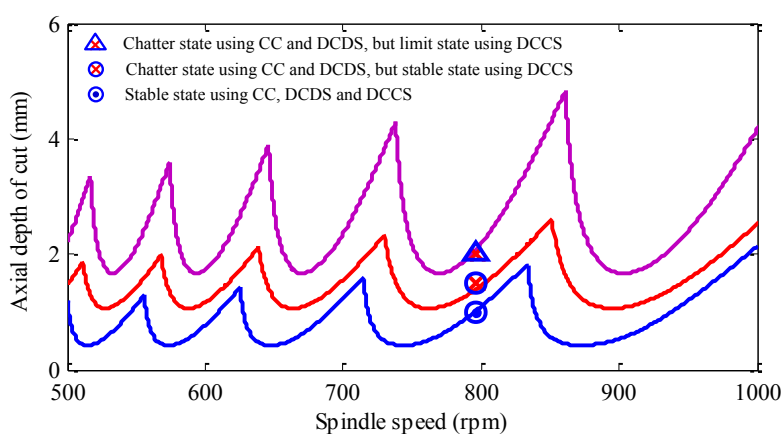


Figure 11. Stability charts for the CC, DCDS and DCCS

When a is equal to 1 mm, the rotational frequency (13.27 Hz) and its multiplication frequencies (39.8 Hz, 53.1 Hz, 79.6 Hz, ...) are the dominant frequency in Figure 12 whether the damping cutters are used or not. This always means that the milling state is stable when using the conventional or damping cutters. When a reaches to 1.5 mm, complex frequencies appear in Figures 13a and 13b. Specifically, the vibration responses gather around 314.3 Hz and 367.5 Hz in Figure 13a. However, these frequencies are not the integral multiple of rotational frequency, and they can be approximately expressed by 314 Hz and 314 Hz plus 4 times of rotational frequency. From modal testing, the first order natural frequency of the conventional cutter along x direction is about 314 Hz, which is not equal to 312 Hz along y direction, since the spindle is not symmetrical. In other words, the responses near natural frequency are dominant, which means the occurrence of chatter. Similarly, it can be found in Figure 13b that the chatter also appears when using the DCDS, while the vibration amplitude is much less than that in Figure 13a. When the DCCS is used, the milling process is still stable as shown in Figure 13c. The axial depth of cut further increases to 2 mm. Compared to Figures 13a and 13b, the chatter phenomenon becomes serious in Figures 14a and 14b when using the CC

and DCDS, respectively. Additionally, it shows the slight unstable in Figure 14c when DCCS is used, where some complex frequencies appear. Under different axial depths of cut, the machining state shows various forms. The measured results agree with the predicted stability charts, which can verify the effectiveness of the damping cutters on chatter stability, especially the DCCS.

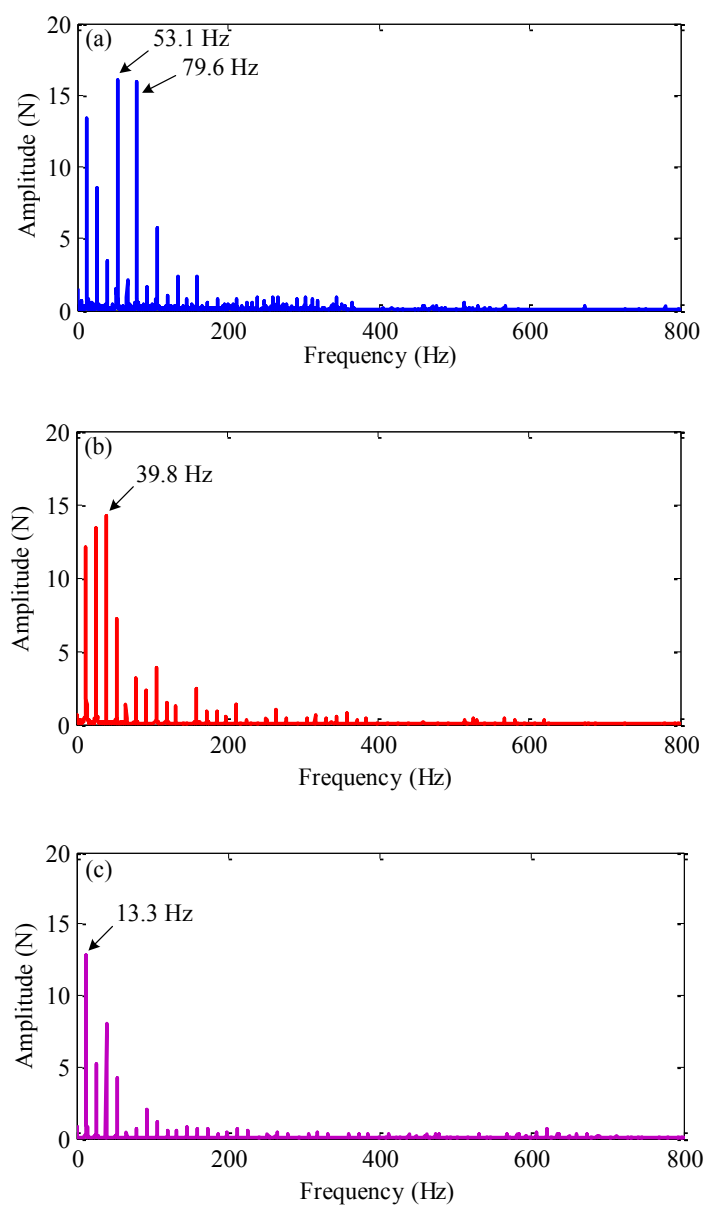


Figure 12. Milling force in frequency domain under $a = 1.0$ mm when using the CC (a), DCDS (b) and DCCS (c).

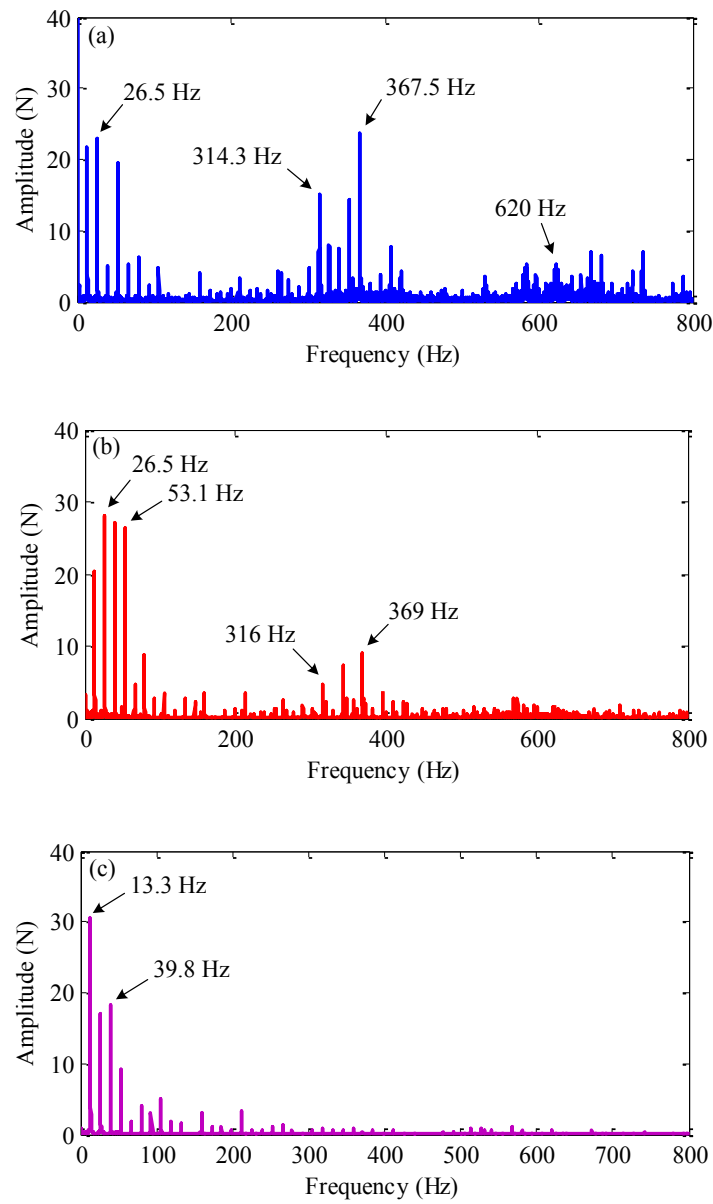
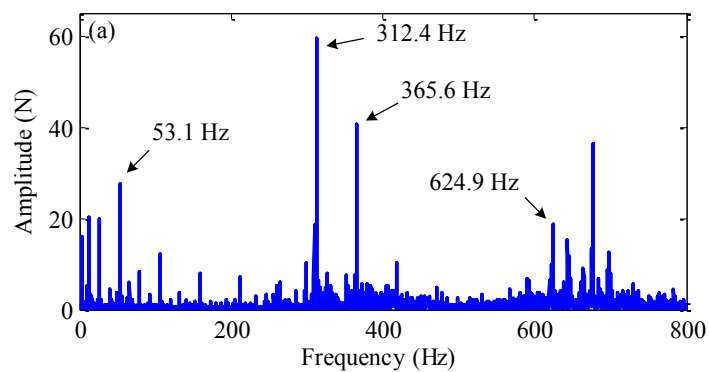


Figure 13. Milling force in frequency domain under $a = 1.5$ mm when using the CC (a), DCDS (b) and DCCS (c).



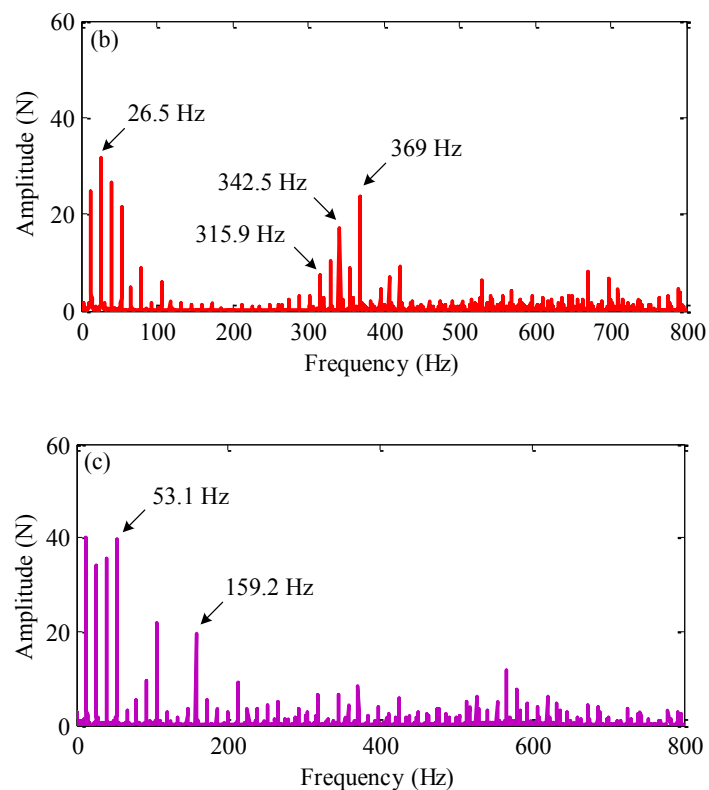


Figure 14. Milling force in frequency domain under $a = 2.0$ mm when using the CC (a), DCDS (b) and DCCS (c).

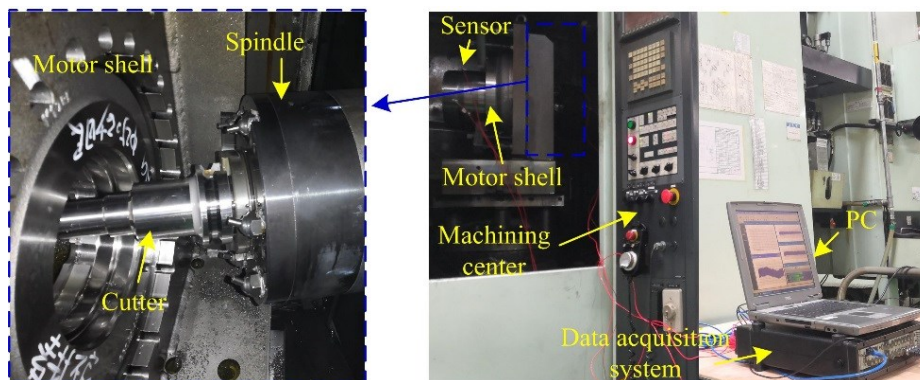


Figure 15. Vibration acceleration signal acquisition under the actual milling process.

In order to further compare the machining performance, the damping cutters are then used to machine the motor shell in workshop as shown in Figure 15. The cutting parameters of the conventional cutter used in workshop are selected. The corresponding acceleration responses are acquired via the acceleration sensor during milling process. The measured results are shown in Figure 16. It can be found that the chatter occurs when using the CC and DCDS, but the amplitude in Figure 16b is far below that in Figure 16a. Meantime, the machining state is stable when using

the DCCS. These imply that the performance of the chatter control in the order from high to low is DCCS, DCDS and CC.

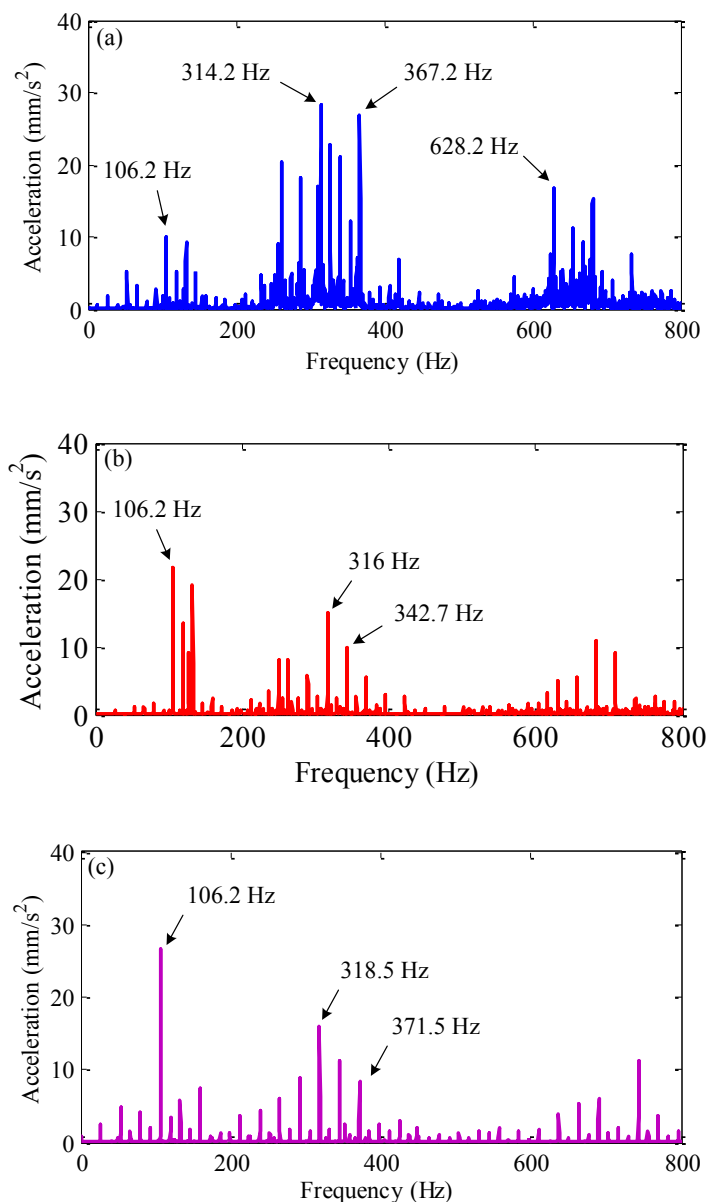


Figure 16. Vibration acceleration responses under $a = 1.5$ mm when using the CC (a), DCDS (b) and DCCS (c).

5. Conclusions

This work investigates the improvement of stable processing condition for the milling cutter with low rigidity. An efficient method is proposed to improve the stable zone by developing the damping cutter based on the passive control method. The dynamic model for the cutter system is

built to reveal the effect of stiffness and loss factor on chatter stability. Then, the damping cutters are designed by embedding the strips and damping core into the toolholder, whose modal characteristics analysis shows that the structural dimension and damping materials have an important effect on the dynamic performance of the damping cutters. After the optimization analysis, two damping cutters with the optimal parameters are manufactured. Modal testing is carried out to compare the dynamic characteristic of the conventional and damping cutters. The measured results show that the dynamic stiffness of the damping cutter with 0.47 MN/m or 0.76 MN/m is much larger than that of the conventional cutter with 0.21 MN/m. The predicted stability charts for three cutters are verified by cutting tests. Comparison with the conventional cutter, the chatter stability is improved significantly when using the damping cutters. It is worth noting that the designed damping cutters have been practically applied to machining the motor shell in the workshop of KSD.

Author Contributions: Conceptualization, Methodology: Yi Wan, Xichun Luo, Zhanqiang Liu; Investigation and data curation: Yan Xia, Yanan Li, Jinglong Cao; Project administration, Supervision: Yi Wan, Ning Gong; Writing—original draft preparation: Yan Xia.

Funding: This research was funded by National Natural Science Foundation of China (Grant No. 51975336), the Key Science and Technology Innovation Project of Shandong Province (Grant No. 2019JZZY010112), Key basic research project of Natural science foundation in Shandong province (Grant No. ZR2018ZB0106), and China Scholarship Council (Grant No. 201906220122).

Acknowledgments: The authors are grateful to the support from Komatsu (Shan Dong) Construction Machinery Co., Ltd. in the manufacture of cutter and experiments

Conflicts of Interest: The authors declare no conflict of interest.

References

1. Liu, Y.; Zhang, D.; Wu, B. An efficient full-discretization method for prediction of milling stability. *Int. J. Mach. Tools Manuf.* **2012**, *63*, 44-48.
2. Quintana, G.; Ciurana, J. Chatter in machining processes: a review. *Int. J. Mach. Tools Manuf.* **2011**, *51*, 363-376.
3. Yue, C.; Gao, H.; Liu, X.; Liang, S.; Wang, L. A review of chatter vibration research in milling. *Chin. J. Aeronaut.* **2019**, *32*, 215-242.
4. Xia, Y.; Wan, Y.; Luo, X.; Wang, H.; Gong, N.; Cao, J.; Liu, Z.; Song, Q. Development of a toolholder with high dynamic stiffness for mitigating chatter and improving machining efficiency in face milling. *Mech. Syst. Signal Process.* **2020**, 106928.

5. Zhang, Z.; Li, H.; Meng, G.; Tu, X.; Cheng, C. Chatter detection in milling process based on the energy entropy of VMD and WPD. *Int. J. Mach. Tools Manuf.* **2016**, 108, 106-112.
6. Albertelli, P.; Braghieri, L.; Torta, M.; Monno, M. Development of a generalized chatter detection methodology for variable speed machining. *Mech. Syst. Signal Process.* **2019**, 123, 26-42.
7. Yao, Y.C.; Chen, Y.H.; Liu, C.H.; Shih, W.P. Real-time chatter detection and automatic suppression for intelligent spindles based on wavelet packet energy entropy and local outlier factor algorithm. *Int. J. Adv. Manuf. Technol.* **2019**, 103, 297-309.
8. Liu, C.F.; Zhu, L. D.; Ni, C. B. Chatter detection in milling process based on VMD and energy entropy. *Mech. Syst. Signal Process.* **2018**, 105, 169-182.
9. Tran, M.Q.; Liu, M.K.; Tran, Q.V. Milling chatter detection using scalogram and deep convolutional neural network. *Int. J. Adv. Manuf. Technol.* **2020**, 107, 1505-1516.
10. Zhu, W.; Zhuang, J.; Guo, B.; Teng, W.; Wu, F. An optimized convolutional neural network for chatter detection in the milling of thin-walled parts. *Int. J. Adv. Manuf. Technol.* **2020**, 106, 3881-3895.
11. Wan, S.; Li, X.; Su, W.; Yuan, J.; Hong, J.; Jin, X. Active damping of milling chatter vibration via a novel spindle system with an integrated electromagnetic actuator. *Precis. Eng.* **2019**, 57, 203-210.
12. Wang, S.; Song, Q.; Liu, Z. Vibration suppression of thin-walled workpiece milling using a time-space varying PD control method via piezoelectric actuator. *Int. J. Adv. Manuf. Technol.* **2019**, 105, 2843-2856.
13. Jiang, X.; Zhao, G.; Lu, W. Vibration suppression of complex thin-walled workpiece based on magnetorheological fixture. *Int. J. Adv. Manuf. Technol.* **2020**, 106, 1043-1055.
14. Merrit, H. Theory of self-excited machine-tool chatter-contribution to machine tool chatter research-1. *ASME J. Eng. Ind.* **1965**, 447-454
15. Insperger, T.; Stépán, G. Updated semi-discretization method for periodic delay-differential equations with discrete delay. *Int. J. Numer. Meth. Eng.* **2004**, 61, 117-141.
16. Ding, Y.; Zhu, L.; Zhang, X.; Ding, H. A full-discretization method for prediction of milling stability. *Int. J. Mach. Tools Manuf.* **2010**, 50, 502-509.
17. Ding, Y.; Zhu, L.; Zhang, X.; Ding, H. Second-order full-discretization method for milling stability prediction. *Int. J. Mach. Tools Manuf.* **2010**, 50(10), 926-932.
18. Altintas, Y.; Stepan, G.; Merdol, D.; Dombovari, Z. Chatter stability of milling in frequency and discrete time domain. *CIRP J. Manuf. Sci. Technol.* **2008**, 1, 35-44.
19. Wang, C.; Zhang, X.; Liu, J.; Yan, R.; Cao, H.; Chen, X. Multi harmonic and random stiffness excitation for milling chatter suppression. *Mech. Syst. Signal Process.* **2019**, 120, 777-792.
20. Madoliat, R.; Hayati, S.; Ghasemi Ghalebahman, A. Investigation of chatter suppression in slender end mill via a frictional damper. *Sci. Iran. B* **2011**, 18, 1069-1077.
21. Liu, X.; Liu, Q.; Wu, S.; Li, R.; Gao, H. Analysis of the vibration characteristics and adjustment method of boring bar with a variable stiffness vibration absorber. *Int. J. Adv. Manuf. Technol.* **2018**, 98, 95-105.
22. Yang, Y.; Wang, Y.; Liu, Q. Design of a milling cutter with large length-diameter ratio based on embedded passive damper. *J. Vib. Control* **2018**, 25, 506-516.
23. Song, Q.; Shi, J.; Liu, Z.; Wan, Y.; Xia, F. Boring bar with constrained layer damper for improving process stability. *Int. J. Adv. Manuf. Technol.* **2016**, 83, 1951-1966.
24. Liu, Y.; Liu, Z.; Song, Q.; Wang, B. Development of constrained layer damping toolholder to improve chatter stability in end milling. *Int. J. Mech. Sci.* **2016**, 117, 299-308.
25. Dai, G.; Hui, Y.; Jin, K. Design and manufacture of a carbon fiber epoxy rotating boring bar. *Compos. Struct.*

This is a peer-reviewed, accepted author manuscript of the following article: Xia, Y., Wan, Y., Luo, X., Wang, H., Gong, N., Cao, J., ... Liu, Z. (2020). Chatter suppression in large overhang face milling using a toolholder with high dynamic performance. *International Journal of Advanced Manufacturing Technology*, 108, 1713-1724.
<https://doi.org/10.1007/s00170-020-05515-3>

2003, 60, 115-124.

26. Yim J.; Cho S.; Seo Y.; Jang B. A study on material damping of 0 laminated composite sandwich cantilever beams with a viscoelastic layer. *Compos. Struct.* **2003**, 60,367-374.